DECOHERENCE PATTERNS OF TOPOLOGICAL QUBITS

Feng-Li Lin (National Taiwan Normal Univ)

Based on 1603.05136 (JHEP) with Pei-Hua Liu(NTNU)

& 1406.6249 (NJP) with Shi-Hao Ho(NCTS), Sung-Po Chao(NCTS) & Chung-Hsien Chou(NCKU)

Talk @ NTU for Chiral Matter & Topology--- 2018/12/06
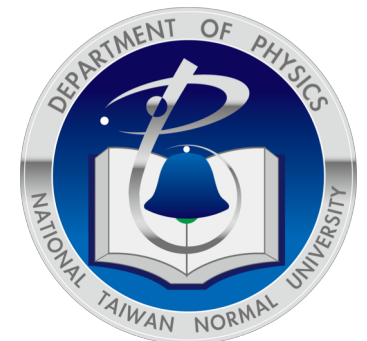
Outline

1. Motivation

2. Majorana zero modes & Topological qubit

3. Reduced dynamics

4. Robust topological qubits

5. Accelerating topological qubit

6. Conclusion

I. Motivation:Topological Order in Open System

Motivation

- Most physical qubits are not robust against quantum decoherence, i.e., leaking its quantum information into the environment.

- The robust qubits play key roles for reliable quantum computations. Looking for robust qubit is a urgent task.

- The fundamental way of making robust qubit not by fine tuning is to implement it based on physical principle.

- One way is to make the qubit topological, i.e., protected by the topological order.

II. Majorana zero mode & Topological qubit

Majorana zero modes (MZMs)

■The Dirac fermion localizing on a topological defect (such as monopole, string or domain wall) results in MZMs. See Jackiw-Rebbi or Jackiw-Rebbi.

■In some sense, a MZM is half of the Dirac fermion, and squares itself to unity. Two different MZMs anti-commute with each other.

$$d_i = (\gamma_{2i-1} + i\gamma_{2i})/2$$

$$\gamma_a^\dagger = \gamma_a \ , \qquad \{\gamma_a, \gamma_b\} = 2\delta_{a,b}$$

$$\{d_i, d_i^\dagger\} = 1$$

Kitaev's chain: 1D superconductor

■The Z_2 1D p-wave superconductor is a model of TSc.

$$H_F = w \sum_{i=1}^{N-1} (d_i - d_{i+1}^\dagger)(d_{i+1} + d_{i+1}^\dagger) + 2v \sum_{i=1}^{N} (d_i^\dagger d_i - 1/2) , \qquad [(-1)^{\sum_i d_i^\dagger d_i}, H_F] = 0$$

■This can be seen by introducing the fractional Majorana fields

$$H_F \sim v \sum_{i=1}^{N} \gamma_{2i-1}\gamma_{2i} + w \sum_{i=1}^{N-1} \gamma_{2i}\gamma_{2i+1}$$

■The edge Majorana modes are robust and protected by Z_2.
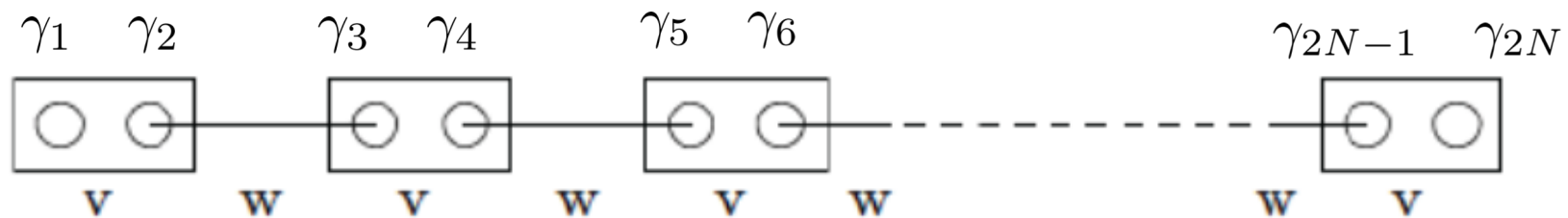
■Two phases: one has no dangling Majorana modes, one does.

Topological Qubit

- We can pair up two spatially separated Majorana zero modes to form a qubit. We call it topological qubit.

- However, this is not really a qubit due to Z2 parity: $i\gamma_1\gamma_2|0\rangle = |0\rangle$, $\qquad i\gamma_1\gamma_2|1\rangle = -|1\rangle$

- Thus, we cannot form a state like $|0\rangle + e^{i\phi}|1\rangle$ as long as Z2 parity is preserved.

Way out

- One way-out is to use 4 MZMs to form one topological qubit by just restricting to the parity even states, e.g., a logical qubit as $a|00\rangle + b|11\rangle$

- Another way-out is to couple the MZMs to the environment so that the MZMs are now open system, which can no longer preserve Z2 parity.

- The 2nd way is what we will consider in this talk. So, 2 MZMs make one topological qubit.

Fermionic or Bosonic environments

■In this work, we consider two ways of coupling the Kitaev's chains to the environments:

1. The fermionic channel:

$$\sum_a \gamma_a \mathcal{O}_a \;, \qquad \mathcal{O}^\dagger = -\mathcal{O}_a$$

These interactions breaks the parity symmetry.
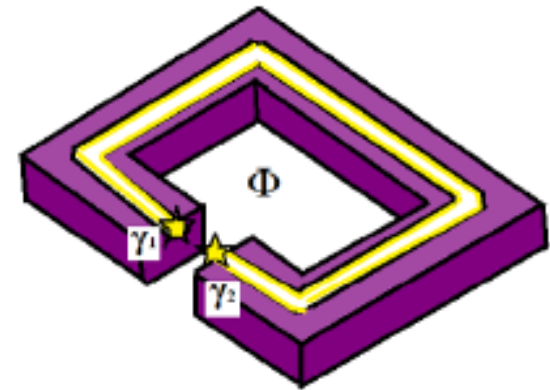
2. The bosonic channel:

$$\gamma_1 \gamma_2 \mathcal{O}_{12} + \gamma_3 \gamma_4 \mathcal{O}_{34} \;, \quad \text{or} \quad \gamma_1 \gamma_3 \mathcal{O}_{13} + \gamma_2 \gamma_4 \mathcal{O}_{24} \;, \qquad \mathcal{O}^\dagger_{ab} = -\mathcal{O}_{ab}$$

These interactions preserve the parity symmetry. We will see this will cause different decoherence patterns from the fermionic ones.

MZMs as Open System

- Hamiltonian: $H_{total} = H_{probe} + H_{env}^{(Ohmic)} + V$

$$H_{probe} = 0 \,, \qquad V = \sum_a B_a \gamma_a \mathcal{O}_a + \sum_{a>b} B_{ab} \gamma_a \gamma_b \mathcal{O}_{ab}$$

- Environment operator, e.g. $\mathcal{O}_a = \psi_a - \psi_a^\dagger \qquad \mathcal{O}_{ab} = \psi_a \psi_b^\dagger$
- They are assumed to Ohmic-type:

$$S_{spec}^{(env)}(\omega) = c_0(Q)\omega^Q \, e^{-\omega^2/\Gamma_0^2} \,, \qquad Q \geq 0$$

- They obey the locality constraint:

$$\langle \mathcal{O}_1(t)\mathcal{O}_2(t') \rangle = 0$$

III. Reduced dynamics

RDM in Interaction picture

$$\rho^D(\tau) = U(\tau)\,\rho_0\,U^\dagger(\tau) \qquad \rho_0 = \rho_{M,0} \otimes |0\rangle_e \langle 0|$$

$$U(\tau) = \mathrm{T}\,e^{-i\int^\tau V^\tau(\tau')d\tau'} \qquad V^\tau := \sum_i \gamma_i\,\mathcal{O}_i^\tau(\tau) \qquad O_i[t,\vec{x}] := e^{iH_E t}\,O_i[\vec{x}]\,e^{-iH_E t}\,.$$

$$\rho_M(\tau) = \mathrm{Tr}_E\,e^{-iH_E^\tau \tau}\,\rho^D(\tau)\,e^{-iH_E^\tau \tau} = \mathrm{Tr}_E\,\rho^D(\tau)\,.$$

- In general, it is difficult to obtain the closed form of RDM.

- It usually needs approximation. A common one is the Markov approximation which leads to Lindblad master equation for RDM.

Derive exact RDM for MZMs (1)

- Use Clifford algebra of MZMs, we get

$$U(\tau) = \mathrm{T}\, e^{-i\sum_{1=1,2} \gamma_i \mathbf{O}_i(\tau)} = \mathcal{T}\, \Pi_{i=1,2}\big(\cosh \mathbf{O}_i(\tau) - i\gamma_i \sinh \mathbf{O}_i(\tau)\big)$$

$$U^\dagger(\tau) = \mathcal{T}^\dagger\, \Pi_{i=1,2}\big(\cosh \mathbf{O}_i(\tau) + i\gamma_i \sinh \mathbf{O}_i(\tau)\big)$$

- Note

$$\mathbf{O}_i(\tau) = \int^\tau d\tau'\, \mathcal{O}_i^\tau(\tau')$$

$$\mathrm{T}\, \gamma_1 \mathbf{O}_1(\tau)\gamma_1 \mathbf{O}_1(\tau) = -\int_0^\tau d\tau_1 \int_0^\tau d\tau_2 [\Theta(\tau_1 - \tau_2)\mathcal{O}_1^\tau(\tau_1)\mathcal{O}_1^\tau(\tau_2) + (\tau_1 \leftrightarrow \tau_2)]$$

$$= -\int_0^\tau d\tau_1 \int_0^\tau d\tau_2\, \mathcal{T}\, \mathcal{O}_1^\tau(\tau_1)\mathcal{O}_1^\tau(\tau_2) := -\mathcal{T}\, \mathbf{O}_1(\tau)\mathbf{O}_1(\tau)\,.$$

bosonic time ordering for O operators!!

Derive exact RDM for MZMs (2)

- Use the above and the locality constraint, we get

$$\rho_M(\tau) = C_1 C_2 \, \rho_{M,0} - S_1 C_2 \, \sigma_1 \rho_{M,0} \sigma_1 - S_2 C_1 \, \sigma_2 \rho_{M,0} \sigma_2 + S_1 S_2 \, \sigma_3 \rho_{M,0} \sigma_3$$

$$C_i = \langle \mathcal{T}^\dagger \cosh \mathbf{O}_i(\tau) \mathcal{T} \cosh \mathbf{O}_i(\tau) \rangle \,, \qquad S_i = \langle \mathcal{T}^\dagger \sinh \mathbf{O}_i(\tau) \mathcal{T} \sinh \mathbf{O}_i(\tau) \rangle \,.$$

- No odd parity terms like $\langle \mathcal{T}^\dagger \sinh \mathbf{O}_i(\tau) \mathcal{T} \cosh \mathbf{O}_i(\tau) \rangle$

- These correlators are bosonic under time ordering, and the closed form can be obtained by Wick contraction.

$$\hat{\mathcal{F}} = e^{\frac{1}{2}\int_0^{\mathcal{T}} d\tau_1 \int_0^{\mathcal{T}} d\tau_2 \langle \mathcal{O}_i(\tau_1)\mathcal{O}_j(\tau_2)\rangle \frac{\delta^2}{\delta\mathcal{O}_i(\tau_1)\delta\mathcal{O}_j(\tau_2)}} : \hat{\mathcal{F}} :$$

$$: \hat{\mathcal{F}} :: \hat{\mathcal{G}} := e^{\int_0^{\mathcal{T}} d\tau_1 \int_0^{\mathcal{T}} d\tau_2 \langle \mathcal{O}_{\mathcal{F}}(\tau_1)\mathcal{O}_{\mathcal{G}}(\tau_2)\rangle \frac{\delta^2}{\delta\mathcal{O}_{\mathcal{F}}(\tau_1)\delta\mathcal{O}_{\mathcal{G}}(\tau_2)}} : \hat{\mathcal{F}}\hat{\mathcal{G}} :$$

$$C_i = \langle \mathcal{T}^\dagger \cosh \mathbf{O}_i(\tau) \mathcal{T} \cosh \mathbf{O}_i(\tau)\rangle.$$

$$C_i = \frac{1}{4}\langle \mathcal{T}^\dagger (e^{\mathbf{O}_i(\tau)} + e^{-\mathbf{O}_i(\tau)}) \mathcal{T} (e^{\mathbf{O}_i(\tau)} + e^{-\mathbf{O}_i(\tau)})\rangle$$

$$= \frac{1}{4} e^{\frac{1}{2}\langle \mathcal{T}^\dagger \mathbf{O}_i(\tau)\mathbf{O}_i(\tau)\rangle + \frac{1}{2}\langle \mathcal{T}\mathbf{O}_i(\tau)\mathbf{O}_i(\tau)\rangle} \langle (: e^{\tilde{\mathbf{O}}_i(\tau)} : + : e^{-\tilde{\mathbf{O}}_i(\tau)} :)(: e^{\mathbf{O}_i(\tau)} : + : e^{-\mathbf{O}_i(\tau)} :)\rangle$$

$$= \frac{1}{4} e^{\frac{1}{2}\langle \mathcal{T}^\dagger \mathbf{O}_i(\tau)\mathbf{O}_i(\tau)\rangle + \frac{1}{2}\langle \mathcal{T}\mathbf{O}_i(\tau)\mathbf{O}_i(\tau)\rangle} (2 e^{\langle \tilde{\mathbf{O}}_i(\tau)\mathbf{O}_i(\tau)\rangle} + 2 e^{-\langle \tilde{\mathbf{O}}_i(\tau)\mathbf{O}_i(\tau)\rangle})$$

$$= \frac{1}{2} e^{\frac{1}{2}\langle \mathcal{T}^\dagger \mathbf{O}_i(\tau)\mathbf{O}_i(\tau)\rangle + \frac{1}{2}\langle \mathcal{T}\mathbf{O}_i(\tau)\mathbf{O}_i(\tau)\rangle}$$

$$(e^{\frac{1}{2}\langle \tilde{\mathbf{O}}_i(\tau)\mathbf{O}_i(\tau)\rangle + \frac{1}{2}\langle \mathbf{O}_i(\tau)\tilde{\mathbf{O}}_i(\tau)\rangle} + e^{-\frac{1}{2}\langle \tilde{\mathbf{O}}_i(\tau)\mathbf{O}_i(\tau)\rangle - \frac{1}{2}\langle \mathbf{O}_i(\tau)\tilde{\mathbf{O}}_i(\tau)\rangle})$$

$$= \frac{1}{2}(e^{2\int^{\mathcal{T}} d\tau_1 \int^{\mathcal{T}} d\tau_2 \overline{G}_{i,sym}(\tau_1-\tau_2)} + 1).$$

Exact RDM for 2 MZMs

$$\rho_M(t) = \begin{pmatrix} \frac{1}{2} + (\rho_{00} - \frac{1}{2})e^{\mathcal{I}_1(t)+\mathcal{I}_2(t)} & e^{\mathcal{I}_2(t)}\mathrm{Re}\,\rho_{01} + ie^{\mathcal{I}_1(t)}\mathrm{Im}\,\rho_{01} \\ e^{\mathcal{I}_2(t)}\mathrm{Re}\,\rho_{01} - ie^{\mathcal{I}_1(t)}\mathrm{Im}\,\rho_{01} & \frac{1}{2} - (\rho_{00} - \frac{1}{2})e^{\mathcal{I}_1(t)+\mathcal{I}_2(t)} \end{pmatrix}$$

$$\rho_M(t=0) = \begin{pmatrix} \rho_{00} & \rho_{01} \\ \rho_{01}^* & 1 - \rho_{00} \end{pmatrix}$$

$$\mathcal{I}_i(t) := 2\int^t d\tau \int^t d\tau' \,\overline{G}_{i,sym}(\tau - \tau')$$

$$\overline{G}_{i,sym}(t - t') = \frac{1}{2}\left(\langle \mathcal{O}_i(t)\mathcal{O}_i(t')\rangle + \langle \mathcal{O}_i(t')\mathcal{O}_i(t)\rangle\right).$$

c.f. $G_{i,sym}(t - t') = \frac{1}{2}\left(\langle \mathcal{O}_i(t)\mathcal{O}_i(t')\rangle - \langle \mathcal{O}_i(t')\mathcal{O}_i(t)\rangle\right)$

IV. Robust topological qubits

Characterizing decoherence

- For qubit systems, the most unambiguous way to characterize quantum decoherence is to check if the reduced density matrix becomes a pointer state or not.

- A particular pointer state is the Gibbs state, i..e, thermalization.

Purity and Concurrence

- If the state of the qubits does not reduce to a pointer state, it means the decoherence is incomplete, and could be further purified. Then we can characterize the purity by

$$\mathcal{P} := Tr\rho_r^2(t)$$

- For two-qubit state, we can characterize the quantum entanglement between the two qubits by concurrence:

$$\mathcal{C}(\rho_r) := max(0, \lambda_1 - \lambda_2 - \lambda_3 - \lambda_4)$$

$\lambda_1, \lambda_2, \lambda_3, \lambda_4$ are the square roots of eigenvalues, in decreasing order, of $\rho_r(\sigma_y \otimes \sigma_x)\rho_r^*(\sigma_y \otimes \sigma_x)$.

- Zero concurrence implies no entanglement, but the state could be still quantum.

For initial state described by $\qquad \rho_P(t=0) = \begin{pmatrix} a_{00} & a_{01} \\ a_{01} & a_{11} \end{pmatrix}$

Recall that $\quad \alpha(t) = e^{2B^2 \int^t d\tau \int^t d\tau' \overline{G}_{sym}(\tau-\tau')} = e^{-2B^2|\alpha_{1,2}|I_Q(t;\mu=0,\Gamma_0)}$

Bosonic environments:

$$\rho_r^b(t) = \begin{pmatrix} a_{00} & a_{01}\alpha(t) \\ a_{10}\alpha(t) & a_{11} \end{pmatrix} \qquad\qquad V = \sum_a B_a \gamma_a \mathcal{O}_a + \sum_{a>b} B_{ab}\gamma_a\gamma_b\mathcal{O}_{ab}$$

Fermionic environments:

$$\rho_r^f(t) = \frac{1}{2}\begin{pmatrix} 1+(2a_{00}-1)\alpha^2(t) & 2a_{01}\alpha(t) \\ 2a_{10}\alpha(t) & 1+(2a_{11}-1)\alpha^2(t) \end{pmatrix}$$

Diagonal elements in bosonic environments protected by (fermion) parity so that the qubit state decohere completely but does not thermalize for sub-Ohmic environment. This is not case for the fermionic one.

Special features

- There is no retarded Green function appearing in the final form of the reduced dynamics. This is related to the fact that the Majorana modes are dissipationless, i.e., generating no heat.

- The symmetric Green function appearing above is the Majorana-dressed one as discussed. It control the overall time dependence.

- Turn out that this time factor for Ohmic-like spectrum has a closed form, and has a critical point at Q=1.

$$S_{spec}^{(env)}(\omega) = c_0(Q)\omega^Q \, e^{-\omega^2/\Gamma_0^2} , \qquad Q \geq 0$$

$(Q = 2\kappa - 1$ for fermionic and $Q = 2\Delta - 4$ for bosonic environment)

$Q > 1$ (super Ohmic) $\qquad Q \leq 1$ (Ohmic and sub-Ohmic)
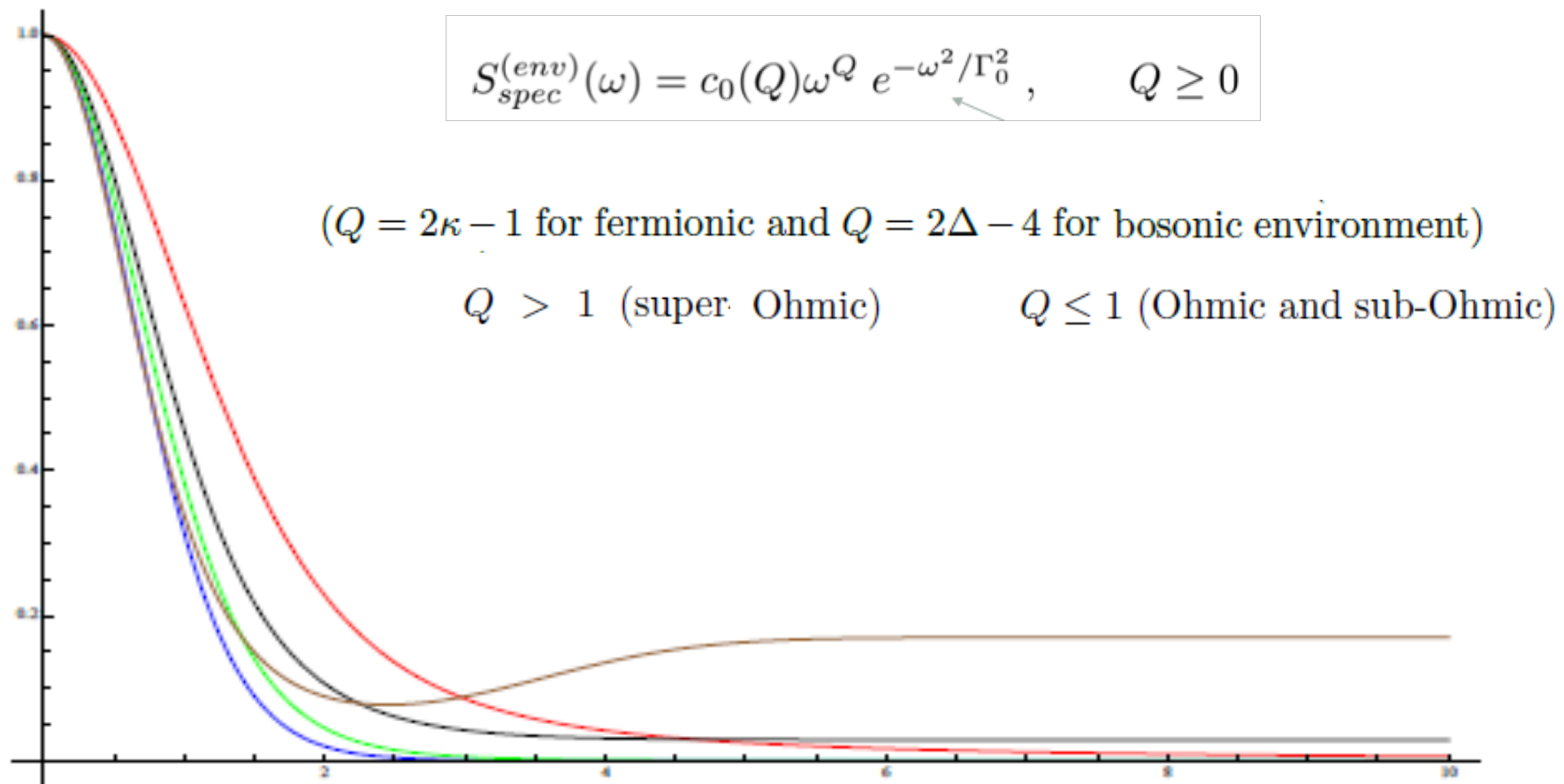
FIG. 3: $e^{-I_Q(t;\mu=0,\Gamma_0=1)}$ v.s. t for $Q = 0.5$(blue), 0.9(green), 1(red), 2 (black) and 4 (brown). This factor controls the time dependence of the influence functional. We can see that there is a critical value at $Q = 1$ beyond which this factor will have a pattern of drop-dip-flat and will not decay to zero.

Effective gap-ness

$$S_{spec}^{(env)}(\omega) = c_0(Q)\omega^Q \, e^{-\omega^2/\Gamma_0^2}, \qquad Q \geq 0$$
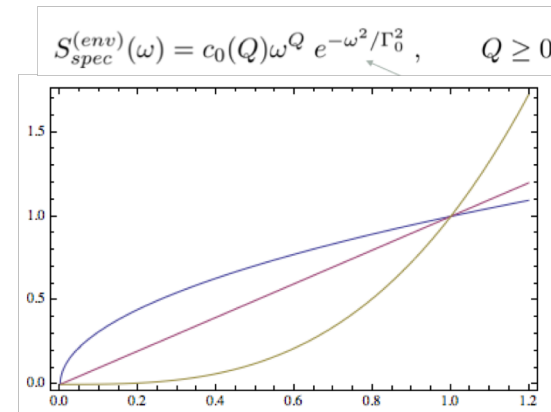
- The quantum information of the probe is carried away by the collective excitations of the environment, which is specified by the spectral density.

- The Ohmic-like spectrum has no gap at low energy, and one would expect the complete decoherence.

- However, the super-Ohmic spectrum suppress more the low energy modes than the higher energy ones.

- Adding the topological nature of the Majorana modes, we see an effective gap emerging for super-Ohmic cases.

Before studying the reduced dynamics for more general initial states:

$$|(e_1, e_2, e_3, e_4)\rangle = e_1|00\rangle + e_2|01\rangle + e_3|10\rangle + e_4|11\rangle$$

with $|e_1|^2 + |e_2|^2 + |e_3|^2 + |e_4|^2 = 1.$

Let us first consider a simple case: choose the initial state as $|(e_1, 0, 0, e_4)\rangle$, i.e.,

$$\rho_P(t=0) = \begin{pmatrix} |e_1|^2 & 0 & 0 & e_1 e_4^* \\ 0 & 0 & 0 & 0 \\ 0 & 0 & 0 & 0 \\ e_1^* e_4 & 0 & 0 & |e_4|^2 \end{pmatrix}$$

Fermionic:
$$\rho_r^f(t) = \frac{1}{4}\begin{pmatrix} A_{11} & 0 & 0 & A_{14} \\ 0 & A_{22} & 0 & 0 \\ 0 & 0 & A_{33} & 0 \\ A_{41} & 0 & 0 & A_{44} \end{pmatrix}$$

with $A_{11} = 1 + \alpha(t)^4 + 2(2|e_1|^2 - 1)\alpha(t)^2$, $A_{22} = A_{33} = 1 - \alpha(t)^2$,

$A_{44} = 1 + \alpha(t)^4 + 2(2|e_4|^2 - 1)\alpha(t)^2$ and $A_{14} = A_{41}^* = 4e_1 e_4^* \alpha(t)^2$

Bosonic:
$$\rho_r^b(t) = \begin{pmatrix} |e_1|^2 & 0 & 0 & e_1 e_4^* \alpha(t)^2 \\ 0 & 0 & 0 & 0 \\ 0 & 0 & 0 & 0 \\ e_1^* e_4 \alpha(t)^2 & 0 & 0 & |e_4|^2 \end{pmatrix}$$

Again, diagonal elements in bosonic environments protected by (fermion) parity.

Two qubits in fermionic environments I
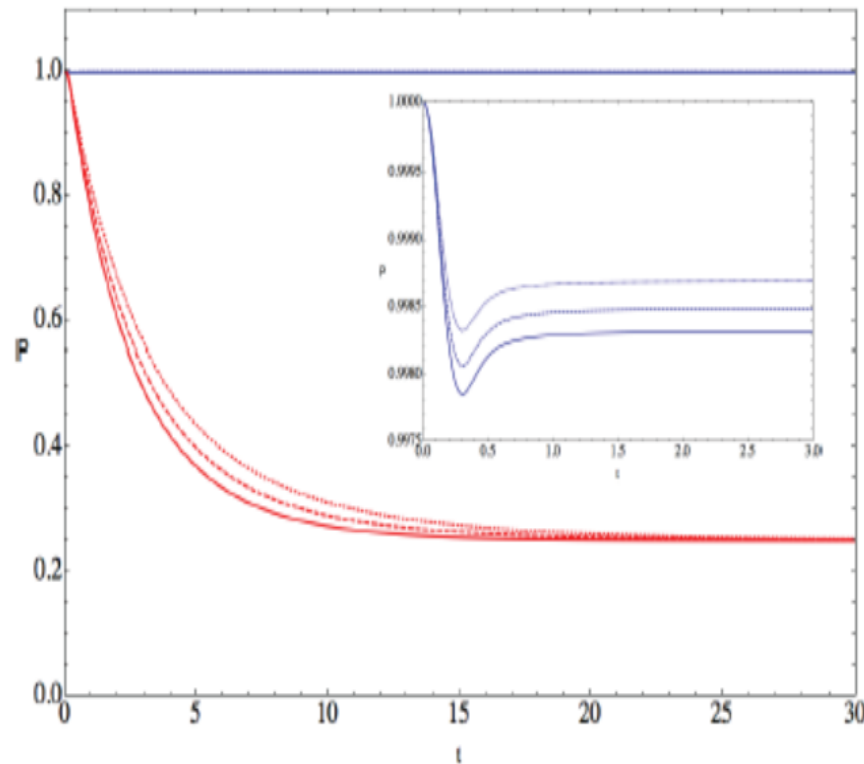
FIG. 4: Purity vs t for $\kappa = 0.5$ (red) and $\kappa = 2$ (blue) w initial states $|(e_1, e_2, e_3, e_4)\rangle = |(1, 0, 0, 1)\rangle$ (solid), $|(2, 1, 0,$ (dashed), $|(1, 1, 0, 1)\rangle$ (dotted). The inset is to magnify early time region of $\kappa = 2$ cases.
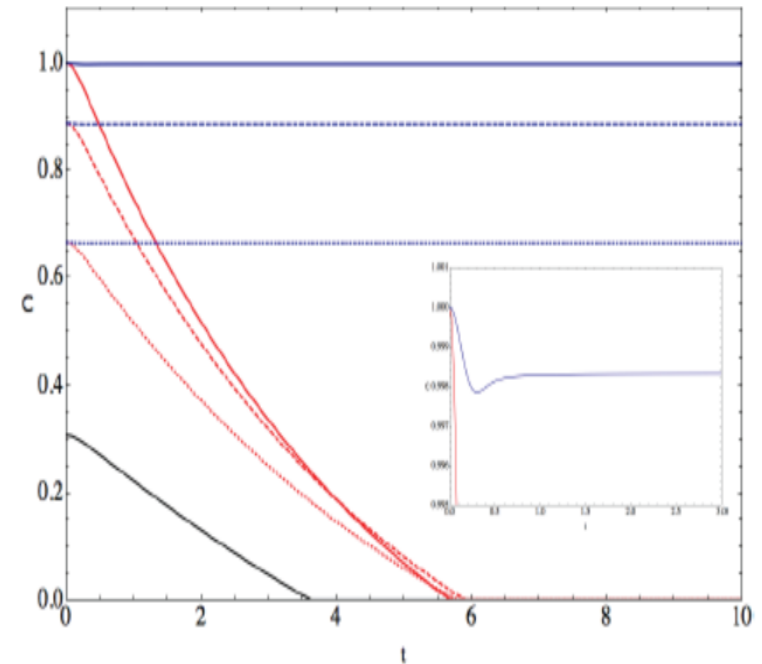
FIG. 5: Concurrence vs t for the states and environments specified in Fig. 4. The inset shows the solid lines enlarged at short time. Here we add a black solid line representing the concurrence pattern of the initial state $|(e_1, e_2, e_3, e_4)\rangle = |(2, 2, 1, 2)\rangle$ in the $\kappa = 0.5$ environment to show its concurrence does not diminish with the other red lines at the same time.

Two qubits in bosonic environments II

The red lines all turn into the pointer states but the blue lines do not.
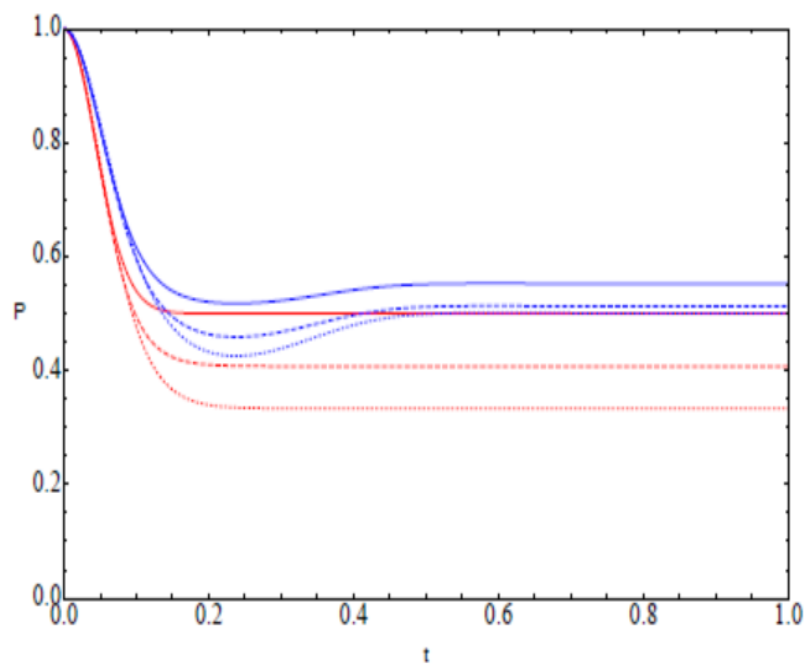
FIG. 6: Purity vs t for $\Delta = 2.3$ (red) and $\Delta = 4.1$ (blue) with initial states $|(e_1, e_2, e_3, e_4)\rangle = |(1, 0, 0, 1)\rangle$ (solid), $|(2, 1, 0, 2)\rangle$ (dashed), $|(1, 1, 0, 1)\rangle$ (dotted).
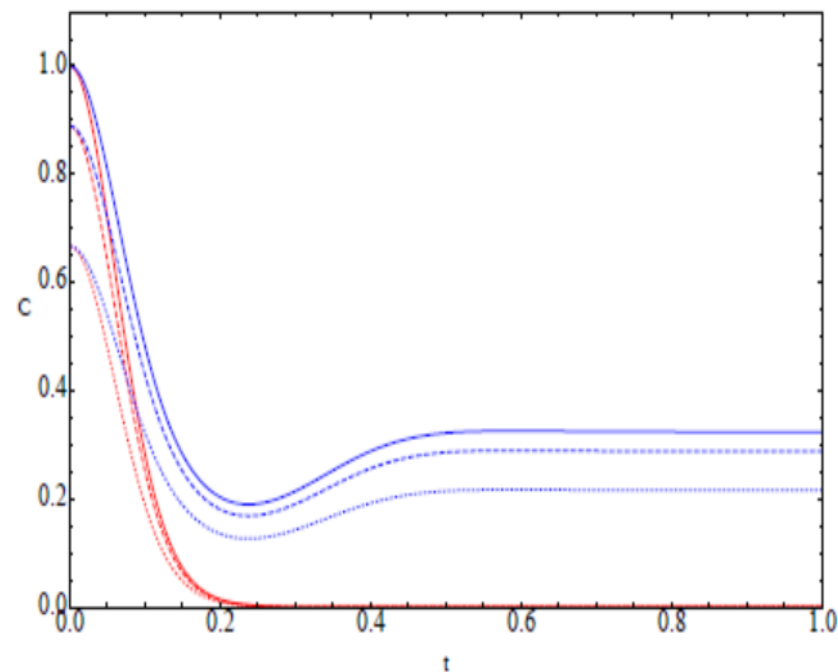
FIG. 7: Concurrence vs t for the states and environments specified in Fig. 6.

Parity-violating bosonic environments

■ In the above, we mainly consider the parity-preserving bosonic environments, i.e.,

$$\gamma_1\gamma_2\mathcal{O}_{12} + \gamma_3\gamma_4\mathcal{O}_{34}$$

■ For the parity-violating ones, i.e., $\gamma_1\gamma_3\mathcal{O}_{13} + \gamma_2\gamma_4\mathcal{O}_{24}$

$$\rho_r^b(\infty) = \begin{pmatrix} \frac{|e_1|^2+|e_4|^2}{2} & 0 & 0 & 0 \\ 0 & \frac{|e_2|^2+|e_3|^2}{2} & 0 & 0 \\ 0 & 0 & \frac{|e_2|^2+|e_3|^2}{2} & 0 \\ 0 & 0 & 0 & \frac{|e_1|^2+|e_4|^2}{2} \end{pmatrix}$$

for sub-Ohmic environment

Only for particular set of initial states, it will be thermalized.

C.f. Spin-Boson model
ref. S.T. Wu PRA89p034301
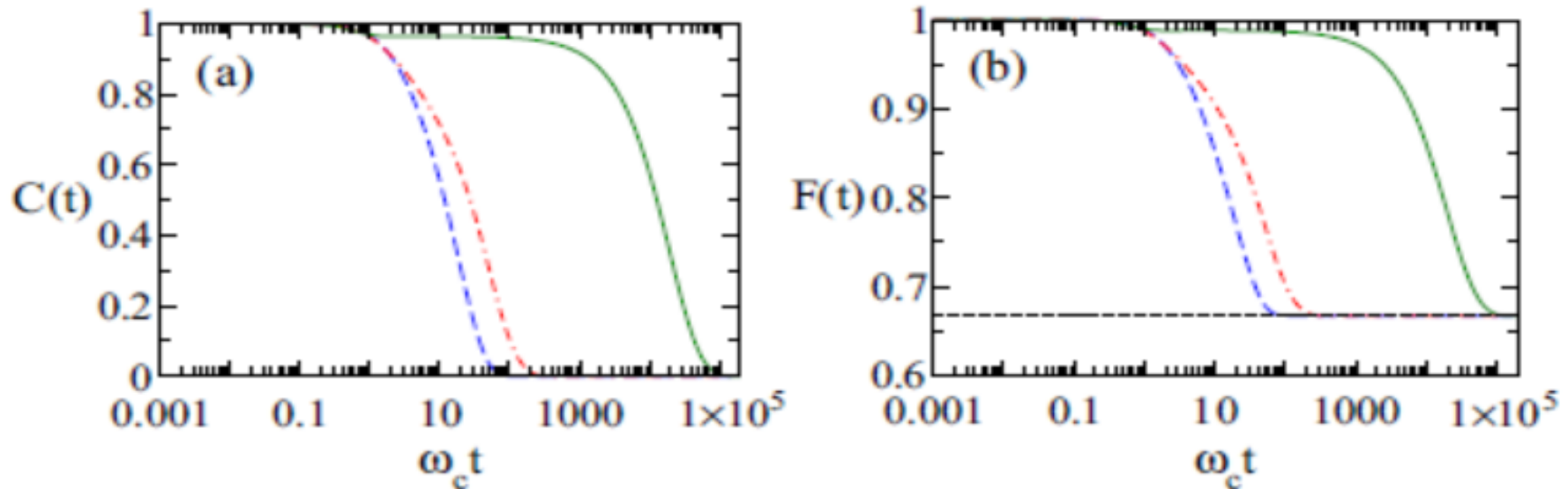
FIG. 3. (Color online) Time evolution for the (a) concurrence and (b) maximum teleportation fidelity for the Bell state (12) at weak environment coupling ($\eta_0 = 0.01$) when the spectral function is sub-Ohmic ($s = 1/2$, blue dashed curves), Ohmic ($s = 1$, red dot-dashed curves), and super-Ohmic ($s = 3$, green solid curves). The horizontal dashed line in (b) indicates the classical limit $F = \frac{2}{3}$.

V. Accelerating topological qubit

MZMs in motion

- We can generalize the above to the MZMs in motion, either boost or in acceleration.
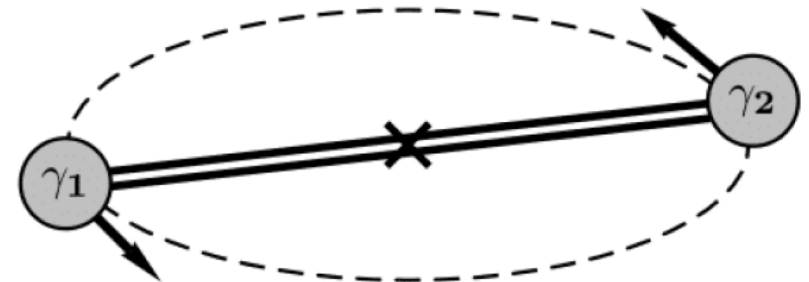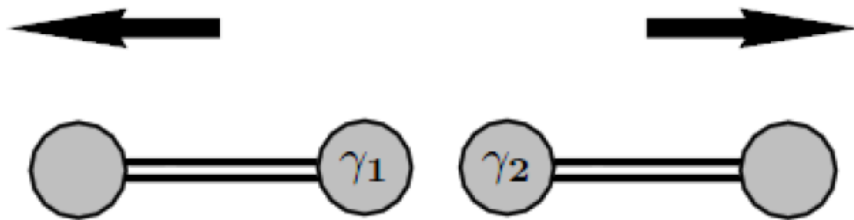
Frame of MZMs (M-frame)   vs   Frame of Environment (E-frame)

Local frame change

- The overall RDM formalism is the same as for the static case.
- Only thing to take care is the change of the local time frame according to the relative motions.

Given local times for MZMs

$$t = t(\tau_i) , \qquad \vec{x} = \vec{x}(\tau_i)$$

$$H_T^{D,\tau_k} = H_E^{\tau_k} + V^{\tau_k}$$

$$H^{\tau_k} := \frac{dt(\tau_k)}{d\tau_k} H_E$$

$$V^{\tau_k} := \lambda_k[\tau_k] \, \gamma_k \, O_k[t(\tau_k), \vec{x}(\tau_k)] + \sum_{i \neq k} \frac{d\tau_i(t(\tau_k))}{d\tau_k} \lambda_i[\tau_i(t(\tau_k))] \, \gamma_i \, O_i[t(\tau_k), \vec{x}(\tau_i(t(\tau_k)))]$$

$$:= \sum_i \gamma_i \, \mathcal{O}_i^{\tau_k}(\tau_k) .$$

Influence functionals in local frames

$$\rho_M(t) = \begin{pmatrix} \frac{1}{2} + (\rho_{00} - \frac{1}{2})e^{\mathcal{I}_1(t)+\mathcal{I}_2(t)} & e^{\mathcal{I}_2(t)}\mathrm{Re}\,\rho_{01} + ie^{\mathcal{I}_1(t)}\mathrm{Im}\,\rho_{01} \\ e^{\mathcal{I}_2(t)}\mathrm{Re}\,\rho_{01} - ie^{\mathcal{I}_1(t)}\mathrm{Im}\,\rho_{01} & \frac{1}{2} - (\rho_{00} - \frac{1}{2})e^{\mathcal{I}_1(t)+\mathcal{I}_2(t)} \end{pmatrix}$$

$$t(\tau) = \frac{\sinh a\tau}{a}, \qquad x(\tau) = \frac{\cosh a\tau - 1}{a}$$

Worldline of constant a!

- Influence functional in M-frame:

$$\mathcal{I}_i^{M_k}(\tau_k) = -2\int_0^{\tau_k} d\tau_k' \int_0^{\tau_k} d\tau_k'' \,\lambda_i(\tau_i(\tau_k'))\lambda_i(\tau_i(\tau_k'')) \int_{-\infty}^{\infty} d\omega \,|\omega|^{d-1}\mathcal{A}_i(\omega)e^{-i\omega(t(\tau_k')-t(\tau_k''))}$$

$$\times \oint d\mathbf{\Omega}\exp\left[i\omega\hat{n}\cdot(\vec{x}(\tau_k') - \vec{x}(\tau_k''))\right] \tag{3.23}$$

- Influence functional in E-frame:

$$\mathcal{I}_i^E(t) = -2\int_0^t dt' \int_0^t dt'' \,\lambda_i(\tau_i(t'))\lambda_i(\tau_i(t''))\frac{d\tau_i}{dt'}\frac{d\tau_i}{dt''} \int_{-\infty}^{\infty} d\omega \,|\omega|^{d-1}\mathcal{A}_i(\omega)e^{-i\omega(t'-t'')}$$

$$\times \oint d\mathbf{\Omega}\exp\left[i\omega\hat{n}\cdot[\vec{x}_i(\tau_i(t')) - \vec{x}_i(\tau_i(t''))]\right] \tag{3.24}$$

Transition Rate

- Treating the MZMs as kind of Unruh-DeWit detector, then the transition amplitude is

$$A_{i \to f}^{(\mathbf{m})} := \lim_{t \to \infty} \langle f | \langle \mathbf{m} | U(t) | \mathbf{0} \rangle | i \rangle$$

- The full transition probability is

$$P_{i \to f} := \sum_{\mathbf{m}} |A_{i \to f}^{(\mathbf{m})}|^2 = \lim_{t \to \infty} \langle f | \sum_{\mathbf{m}} \langle \mathbf{m} | U(t) | \mathbf{0} \rangle | i \rangle \langle i | \langle \mathbf{0} | U^\dagger(t) | \mathbf{m} \rangle | f \rangle = \lim_{t \to \infty} \langle f | \mathrm{Tr}_E \rho^D(t) | f \rangle \, .$$

- In the current setup, it is

$$P_{0 \to 1} = \lim_{t \to \infty} \frac{1}{2} (1 - e^{\mathcal{I}_1(t) + \mathcal{I}_2(t)})$$

Decoherence → zero transition!

Thermalization

- We find that even for robust topological qubit will be thermalized due to Unruh effect.

FIG. 2. Decoherence patterns (exponential of "influence functionals" vs log of proper time) of a constantly-accelerating topological qubit in various frames in the environments of uniform spectrum (Left) and of super-Ohmic spectrum (Right): in the M-frame (solid red), in the E-frame (dotted blue) and of the thermal one (dashed black) with the acceleration $a = 5$.
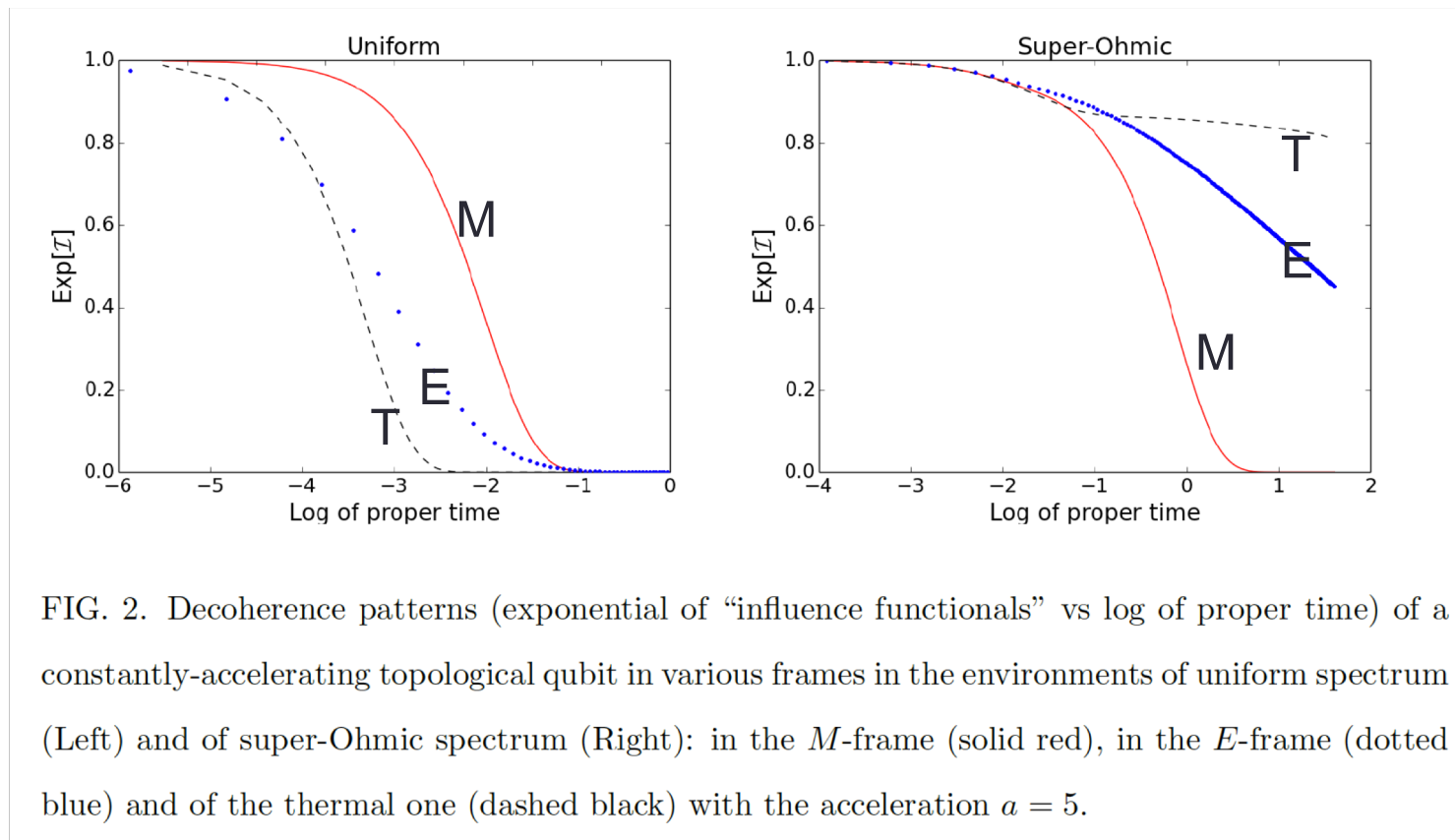
Boosted MZMs
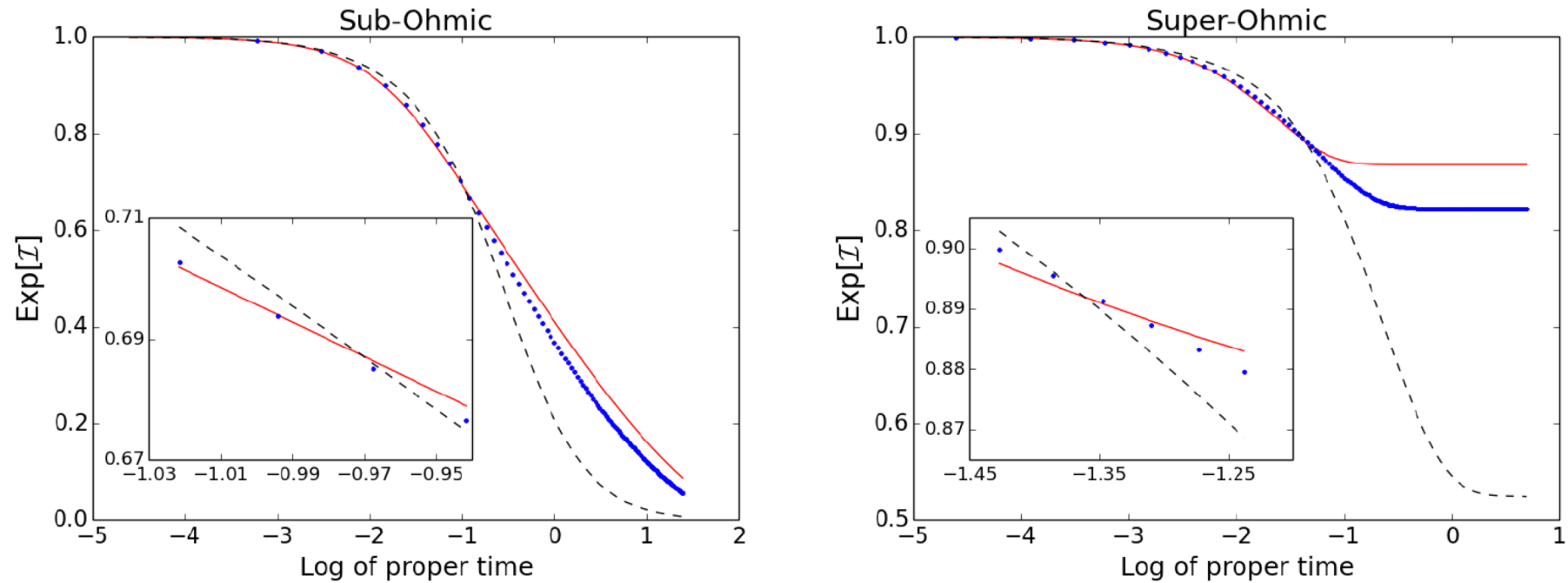
FIG. 4. Decoherence patterns of a boost topological qubit in the M-frame in the environments of sub-Ohmic spectrum (Left panel) and of super-Ohmic spectrum (Right panel) for different velocities: $v = 0$ (solid red), $v = 0.4$ (dotted blue) and $v = 0.8$ (dashed black). The insets show the details of "overtaking" phenomena during the decohrence.

Overtaking/Decoherence inertial impedance
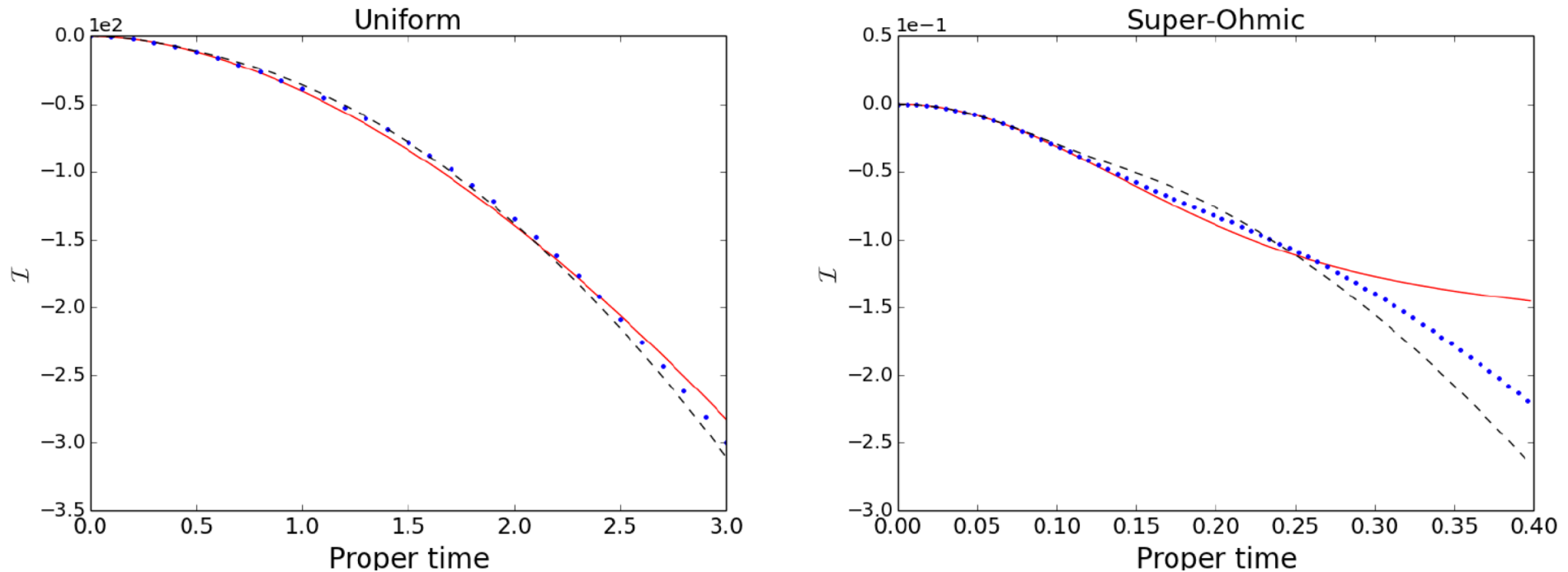
FIG. 3. "Influence functionals" of a constantly-accelerating topological qubit in the M-frame in the environments of uniform spectrum (Left) and of super-Ohmic spectrum (Right) for different accelerations: $a = 1$ (solid red), $a = 5$ (dotted blue) and $a = 10$ (dashed black). Note that the decoherence patterns show the "overtaking" phenomenon.

Anti-Unruh phenomenon (1)

$$\lambda(\tau) = e^{-\frac{\tau^2}{\sigma^2}}$$
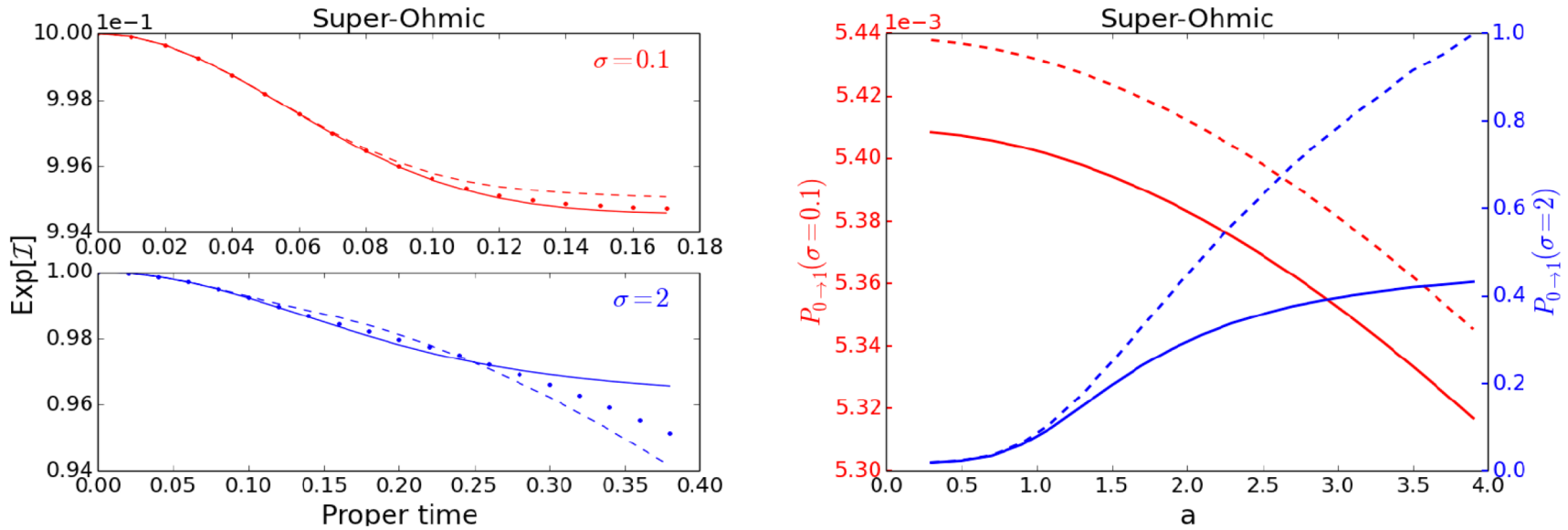
FIG. 5. Decoherence patterns and transition probabilities in the M-frame of a constantly accelerating MUDW detector in the super-Ohmic environment (with $q = 0.5$) with the switching function of the time duration scales: $\sigma = 0.1$ (red) and $\sigma = 2$ (blue). Left : Decoherence patterns with $a = 1$ (solid), $a = 5$ (dashed) and $a = 10$ (dotted). Right: Transition probabilities $P_{0\to1}$ (solid) and $P_{0\to1}^{(1)}$ (dashed) versus acceleration a. The left y-axis is for $P_{0\to1}$ and $P_{0\to1}^{(1)}$ with $\sigma = 0.1$, and the right y-axis with $\sigma = 2$. This figure shows that the "overtaking" and "anti-Unruh" implies each other.

Anti-Unruh phenomenon (2)
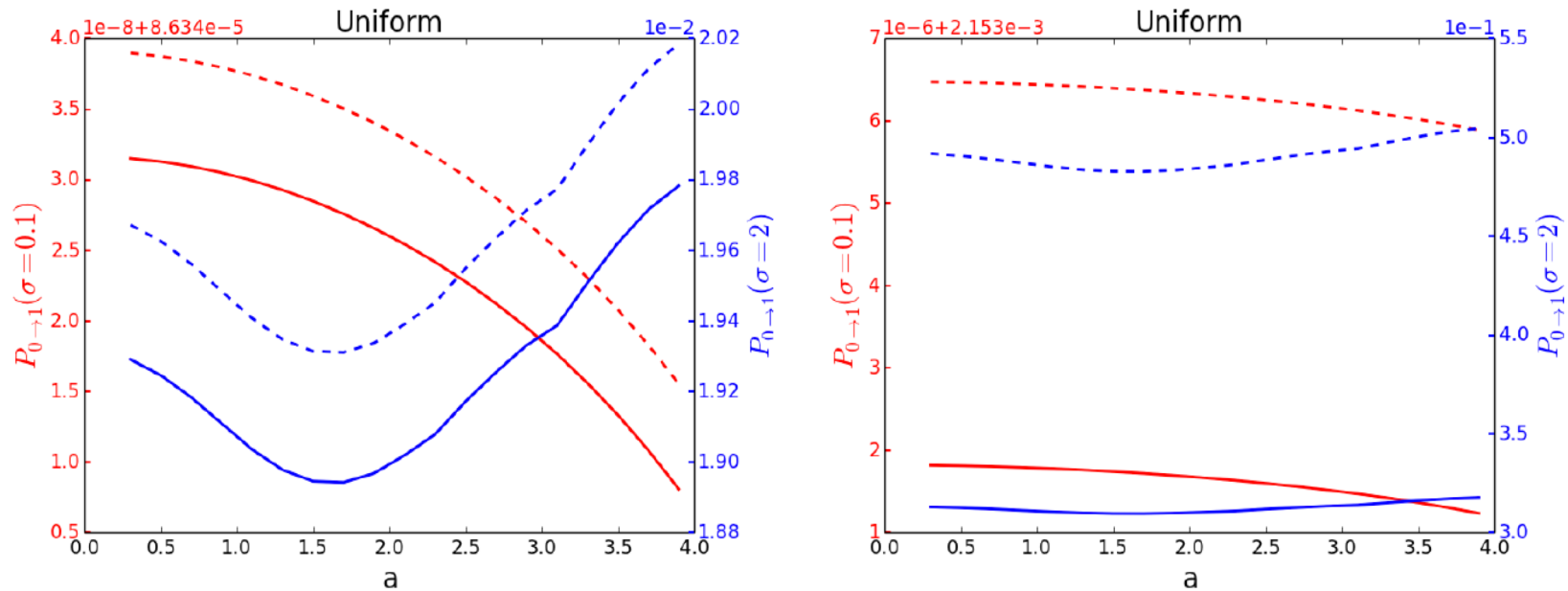
FIG. 6. Transition probabilities $P_{0 \to 1}$ (solid) and $P_{0 \to 1}^{(1)}$ (dashed) in the M-frame of a constantly accelerating MUDW detector with the switching function of the time duration scales: $\sigma = 0.1$ (red) and $\sigma = 2$ (blue) in the environments of uniform spectrum with $q = 0.01$ (Left) and $q = 0.05$ (Right). The IR cutoff $\Lambda_{IR} = 0.02$.

Decoherence inertial impedance

- From the above, we see a highly nontrivial non-equilibrium phenomenon, we call it decoherence inertial impedance.

- There is initial resistance for the system to against the change caused by the external forces such as acceleration.

- That is, the large acceleration cause less decoherence.

- The anti-Unruh and decoherence inertial impedance/overtaking imply each other.

Information backflow: coupling modulation

$$\lambda(\tau) = \cos \omega_M \tau$$
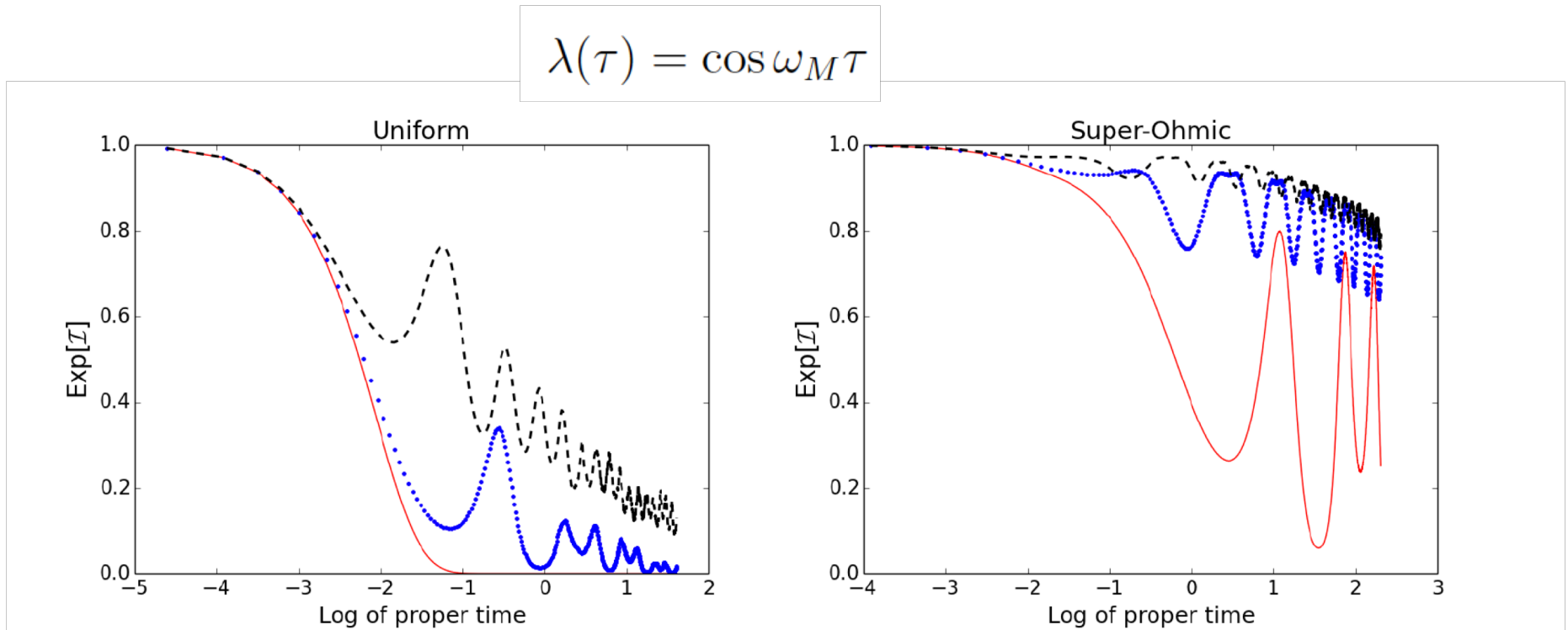
FIG. 9. Decoherence patterns in the M-frame of a constantly accelerating topological qubit in the environments of uniform spectrum (Left) and of super-Ohmic spectrum (Right) with the frequency modulation of the switching function: the modulation frequencies are $\omega_M = 1$ (solid red), $\omega_M = 5$ (dotted blue) and $\omega_M = 10$ (dashed black) with the acceleration $a = 5$.

Information backflow:
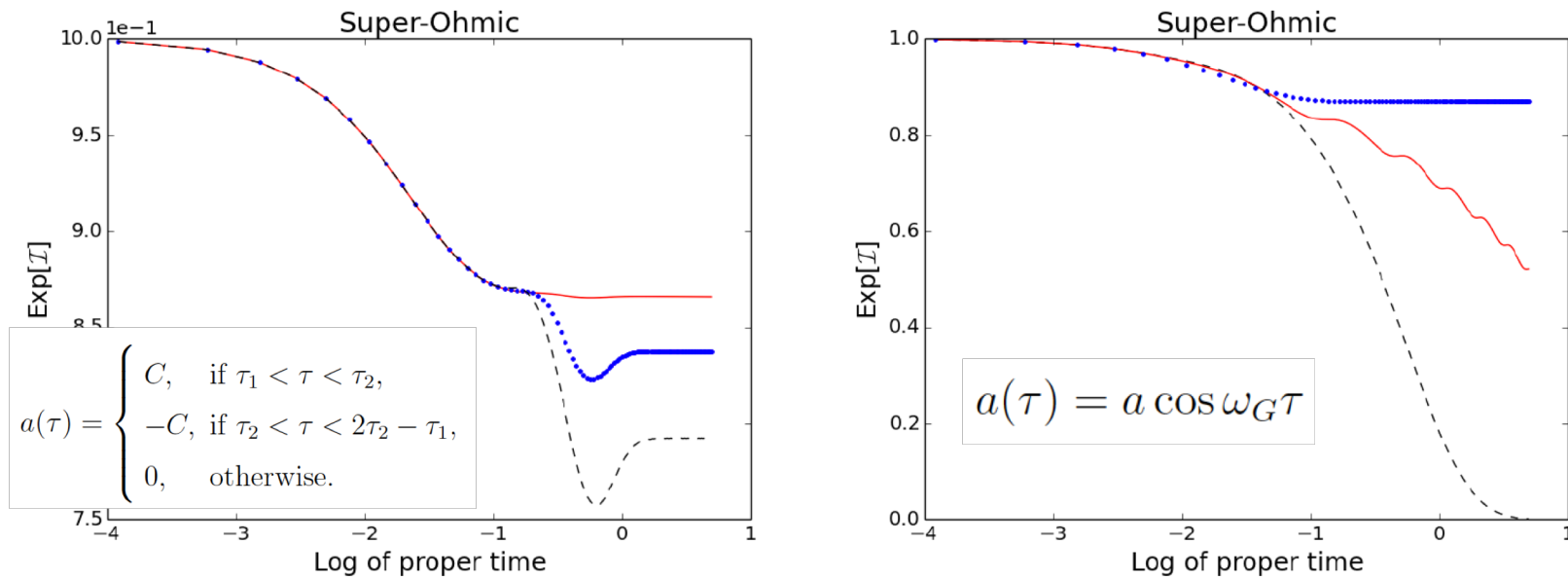
FIG. 10. Decoherence patterns in the M-frame of an accelerating topological qubit in the super-Ohmic environment with the amplitude modulation (AM) and frequency modulation (FM) of the acceleration. Left: AM with $C = 1$ (solid red) , $C = 5$ (dotted blue) and $C = 10$ (dashed black) as $\tau_1 = 0.3$ and $\tau_2 = 0.5$. Right: FM with $\omega_G = 10$ (solid red) , $\omega_G = 50$ (dotted blue) and $\omega_G = 1$ (dashed black) as $a = 10$.

Incoherent motions
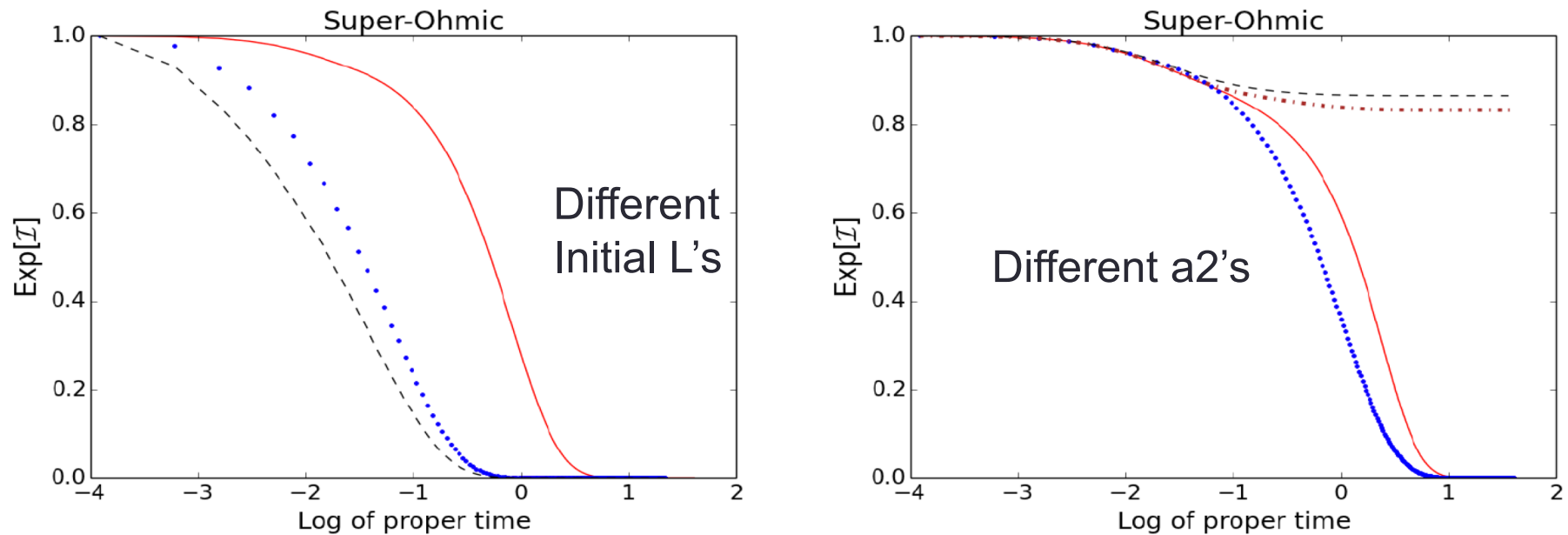
FIG. 11. Decoherence pattern in the super-Ohmic environment associated with the Majorana mode γ_2 moving with the acceleration a_2 as seen from the observer in the comoving frame of the Majorana mode γ_1 moving with the acceleration a. There is an initial separation L between γ_1 and γ_2. Left: $L = 0$ (solid red), $L = 1$ (dotted blue) and $L = 5$ (dashed black) with $a = a_2 = 5$. Right: $a_2 = 5$ (dotted blue), $a_2 = 2$ (solid red), $a_2 = 1$ (dot-dashed brown) and $a_2 = -1$ (dashed black) with $a = 2$ and $L = 0$.

Circular motions

$$t(\tau_i) = \int_0^{\tau_i} \gamma(\tau')d\tau', \quad x(\tau_i) = r_0 \cos\Theta_i(\tau_i), \quad y(\tau_i) = r_0 \sin\Theta_i(\tau_i),$$

$$\Theta_i(\tau_i) := \int_0^{\tau_i} \gamma(\tau')\Omega(\tau')d\tau' + \pi\delta_{i,2}, \quad \gamma(\tau) := \frac{1}{\sqrt{1 - r_0^2\Omega(\tau)^2}}.$$

- We see the similar overtaking, anti-Unruh and information back flow for the circular motions of MZMs.

$$\mathcal{I}_1 = \mathcal{I}_2$$

$$\lambda(\tau) = \cos\omega_M\tau$$
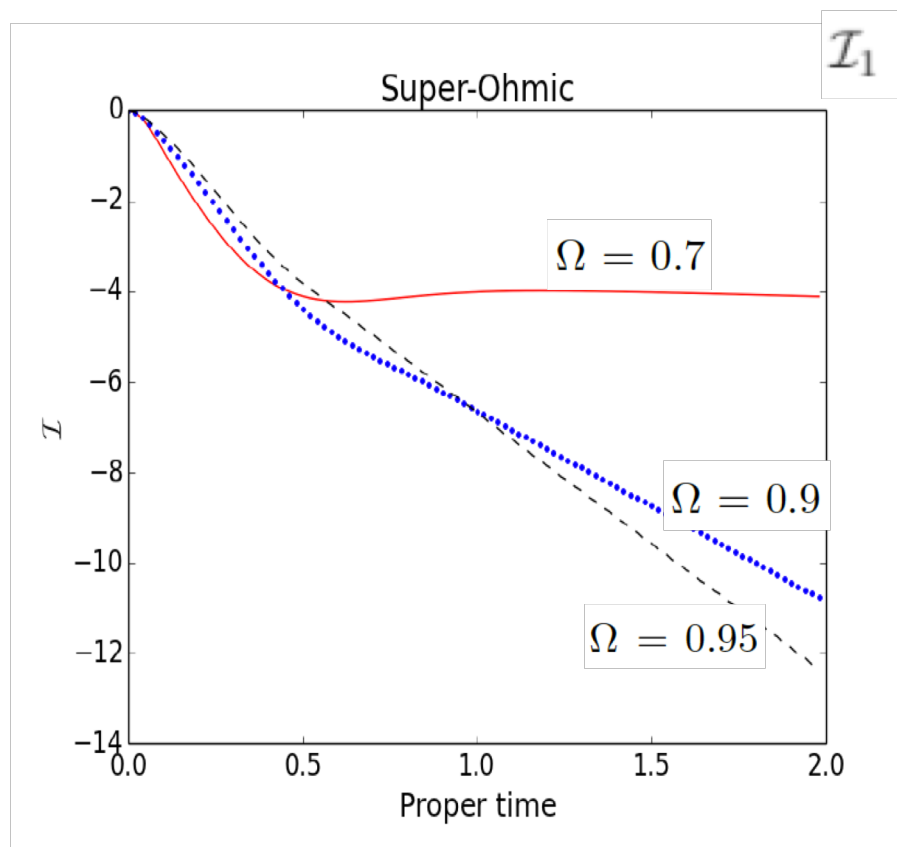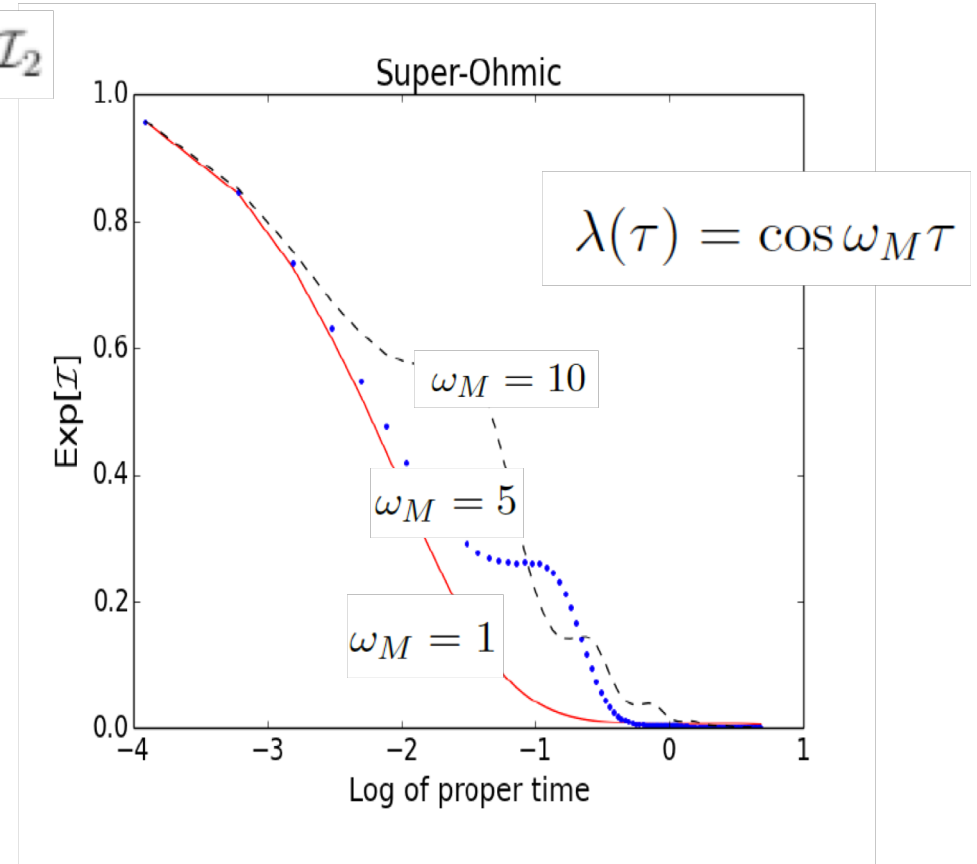
overtaking   backflow

VI. Conclusions

Conlusions

- Our works are the first systematic study of the topological order in open system.
- This is an interesting interplay between topological order and (relativistic) quantum information.
- By the locality constraint, the reduced dynamics can be solved exactly.
- We find the robust topological qubits in the super-Ohmic environment.
- By setting MZMs in motion, we find the universal thermalization, anti-Unruh, decoherence inertial impedance and information backflow.

Thanks!